Advances in Materials Research, *Vol. 13, No. 5 (2024) 375-389*
https://doi.org/10.12989/amr.2024.13.5.375

An experimental study of AAC masonry prisms with chases under compression

Gregoria K. Langstang, Teiborlang Warjri, Richard B. Lyngkhoi and Comingstarful Marthong*

Department of Civil Engineering, National Institute of Technology Meghalaya, Shillong 793003, India

(*Received May 27, 2024, Revised July 20, 2024, Accepted July 24, 2024*)

Abstract. Installing wiring or plumbing fixtures necessitates creating chases within masonry walls, which, while serving practical purposes, raises a crucial concern regarding the potential compromise of the masonry's structural integrity. Given these concerns, it becomes essential to thoroughly understand the impact of incorporating chases on masonry strength. In this study, 37 AAC masonry prisms (200×330×100 mm³) were cast and tested for compression. The prisms were equipped with chases of various depths -10 mm, 20 mm and 30 mm; and orientations (horizontal, inclined, and vertical), which were then filled with mortar using 1:2, 1:4, and 1:6 cement-to-sand ratios. The primary objectives were to assess the strength decrease in the prisms with different chase characteristics compared to a control specimen and to determine the percentage strength increase due to filling materials compared to unfilled chases. Key findings indicate that as chase depth increases, there is a substantial reduction in prism strength. However, the orientation of the chase does not significantly affect strength reduction. Importantly, filling the chases with mortar leads to a significant increase in prism strength. This study not only unveils the complex impact of chase characteristics on masonry strength but also emphasizes the crucial role of filling materials in strengthening these prisms.

Keywords: autoclaved aerated concrete (AAC); chases; compressive strength; failure mode; masonry prisms

1. Introduction

Masonry, as a construction method, holds a distinguished position on a global scale and particularly in India, owing to its myriad advantages that contribute to its widespread usage. Its key attributes such as ready availability of materials, inherent durability, cost-effectiveness, fire protection, thermal and sound insulation (Banerjee *et al.* 2019, Costigan *et al.* 2009, Gumaste *et al.* 2007, Hendry 2001, Sathiparan and Rumeshkumar 2018, Singh and Munjal 2017) have established it as a reliable choice for constructing a wide array of structures. This age-old construction technique not only boasts a rich historical legacy but also showcases a remarkable resilience in adapting to evolving architectural demands, embracing various methods and materials over time. In the context

*Corresponding author, Professor, E-mail: commarthong@nitm.ac.in
[a]Master Student, E-mail: t22ce002@nitm.ac.in
[b]Ph.D. Student, E-mail: p22ce003@nitm.ac.in
[c]Ph.D. Student, E-mail: p21ce005@nitm.ac.in

http://www.techno-press.org/?journal=amr&subpage=5 ISSN: 2234-0912 (Print), 2234-179X (Online)

of masonry's adaptive nature, a notable example is the introduction of Autoclaved Aerated Concrete (AAC) masonry. This innovative material represents a paradigm shift, offering a spectrum of benefits that contribute to its growing popularity in the construction industry, especially in North-east India (Lyngkhoi *et al.* 2023, Raj *et al.* 2020b, a). AAC stands out for its lightweight characteristics, thermal insulation capabilities, durability, and design versatility (Bhosale *et al.* 2019, Ferretti *et al.* 2015, Ferretti and Michelini 2021, Michelini *et al.* 2023, Narayanan and Ramamurthy 2000). Owing to its numerous benefits as a construction material, AAC has gained extensive popularity in masonry construction for various structures (Kałuza 2017).

The necessity to incorporate essential utilities like pipelines and wiring into structures requires the inclusion of chases in walls. Chases, defined as recesses or channels within walls, are crucial for seamlessly accommodating and concealing complex systems such as electrical wiring and plumbing. While serving practical purposes, the introduction of these recesses raises a critical consideration - the potential impact on the structural integrity of the masonry. As chases are carved into walls to house utility elements, changes in the composition and distribution of materials within the wall structure pose questions about overall construction strength and stability. To address these concerns, it is essential to thoroughly understand the impact of incorporating chases on masonry strength, as explored in other studies (Mojsilović 2011, Vicente *et al.* 2014, Al-Sibahy and Edwards 2021, Milani *et al.* 2021, Fleith de Medeiros *et al.* 2022a, b,). For instance, Fleith de Medeiros *et al.* (2022b) examined the stress-strain behavior of small-scale masonry walls with various thicknesses of horizontal chases using numerical simulation with the Lattice Discrete Element Method (LDEM). Fleith de Medeiros *et al.* (2022a) investigated the strength capacity of structural masonry (hollow clay blocks) while considering the effects of chases, evaluated numerically using the Finite Element method (FEM). Mojsilović (2011), Milani *et al.* (2021), Vicente *et al.* (2014) and Al-Sibahy and Edwards (2021) conducted experimental evaluations of the chase effect on masonry walls under compression. Al-Sibahy and Edwards (2021) studied the impact of chases and renovation techniques on masonry wall strength. They found that chases, especially horizontal ones, significantly reduce load-carrying capacity due to stress concentration. Renovation with plastic mesh and cement mortar recovered 55% of lost strength, while galvanized steel channels with mesh and mortar recovered 93%. However, an identified gap in these studies is the limited exploration of diverse materials, specifically, considerations for various types of bricks and filling materials. The studies predominantly focused on traditional masonry elements, emphasizing the need to investigate the potential influence of material variations on structural behavior. Given the increasing prevalence of AAC (Autoclaved Aerated Concrete) blocks in construction practices both in India and globally, there arises a crucial need to investigate how AAC masonry responds to varying load conditions. Understanding the behavior of AAC masonry in the presence of chases, especially under compression, is crucial for informed decision-making in contemporary construction practices. This knowledge gap underscores the necessity to broaden the scope of research to encompass different materials and filling compositions, providing a more comprehensive understanding of the dynamic interactions between AAC blocks, chases, and loading conditions. Such an expanded perspective will significantly contribute to advancing the knowledge base in structural engineering and aiding the effective utilization of AAC blocks in diverse construction scenarios. In construction design, finding the right balance between incorporating utilities and maintaining structural strength is crucial. Assessing the strength implications of integrating chases becomes vital to ensure that the built environment not only fulfills functional needs but also meets rigorous standards of safety and durability. The Indian standard code IS 1905 (1987) specifies that chases are acceptable if they do not compromise the structure's strength and stability, and preference should be given to vertical

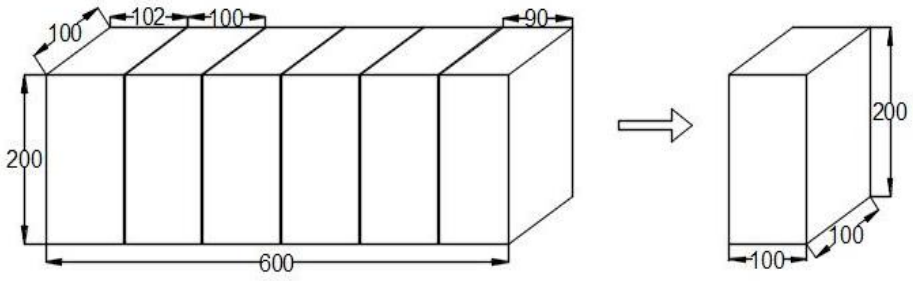

Fig. 1 Schematic diagram of AAC blocks (Note: All dimensions are in mm.)

chases over horizontal ones. The European code EN 1996-1-1 Eurocode 6 provides defined limits for chases, and if these limits are exceeded, the structure's integrity should be carefully considered.

2. Experimental programme

2.1 Materials

For this study, locally sourced AAC blocks measuring 600×200×100 mm³ (l×h×w) were procured. However, these blocks were unsuitable for prism casting at this size; hence, a meticulous cutting process was undertaken, dividing the AAC blocks into six pieces as shown in Fig. 1. This cutting procedure was carried out using a BOSCH tile cutter and an AAC hacksaw. To make up for the loss in thickness during cutting, the blocks were initially marked at 102 mm. After the cutting process, each AAC block produced five desired AAC bricks, and one additional brick with a width of 90 mm was discarded. Consequently, the final AAC bricks were of size 200×100×100 mm³ (l×h×w). Fig. 1. illustrates the schematic diagram of AAC blocks before and after the cutting process.

Moving forward to the mortar mix preparation, fine aggregate conforming to IS:383 (1970) standards, passing through a 4.75 mm sieve, and Pozzolana Portland Cement (PPC) were employed. These materials were obtained from a local merchant. Three types of mortar mixes were utilized, each with distinct cement-to-sand ratios (1:2, 1:4, and 1:6) and a cement-water ratio ranging from 0.45 to 0.5. However, for this study, these mixes were specifically used as filling materials for grooves carved into prisms while only the 1:4 ratio was employed as the binding material. Three mortar cubes for each mixture underwent compression testing according to IS 4031 (Part 6) (1988). The resulting compressive strengths of the materials used are detailed in Table. 1. To simplify notation in this research, the mortar with ratios 1:2, 1:4, and 1:6 are denoted as S (strong), M (moderate strength), and W (weak) mortar respectively.

2.2 Specimen preparation

Masonry prisms, with dimensions of 200 mm×330 mm×100 mm (l×h×w) as shown in Fig. 2, were created by stacking 3 AAC bricks together as depicted in Fig. 3. To enhance adhesion, a cement slurry paste was applied to the bricks as shown in Fig. 3(a) (Raj *et al.* 2020a). A 1:4 mortar mix served as the binding material, and the thickness of the binding mortar was consistently maintained at 15 mm.

Table 1 Compressive strength of materials used

Material	Mortar			AAC blocks
	S	M	W	
Compressive strength (MPa)	27.18	9.15	4.90	2.79

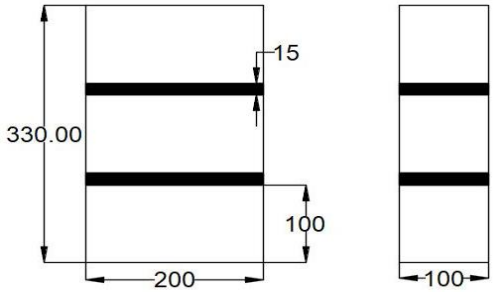

Fig. 2 Dimensions of Test specimens (Note: All dimensions are in mm.)

(a) (b) (c)

Fig. 3 Casting of prism specimen (a) Cement slurry application, (b) Binding mortar application and (c) Casted specimen

Following the casting process, these specimens underwent a curing period of 28 days. Subsequently, chases were cut into the prisms using a tile cutter, with varied depths—10 mm, 20 mm, and 30 mm—and a consistent width of 30 mm. According to Eurocode EN 1996-1-1:2005, chase depths are limited to a maximum of 30 mm, and a 10 mm depth is rarely used due to its impracticality in real-world scenarios. However, the code permits such variations for experimental purposes. This study uses a 10 mm depth primarily as a theoretical investigation to understand its implications on the structural behavior of prisms. Additionally, it facilitates a comparative analysis of different chase depths, highlighting the effects of minor variations on structural performance.

Alongside the depth variations, the chases were cut into three different orientations— horizontal, vertical, and inclined as shown in Fig. 4; aimed at gaining insights into how the structural integrity is influenced by these diverse arrangements. The purpose of incorporating these diverse orientations is to comprehensively understand the impact of differently aligned chases on the overall integrity of the structure. The horizontal, vertical, and inclined chases are denoted by letters H, V and I respectively throughout this paper.

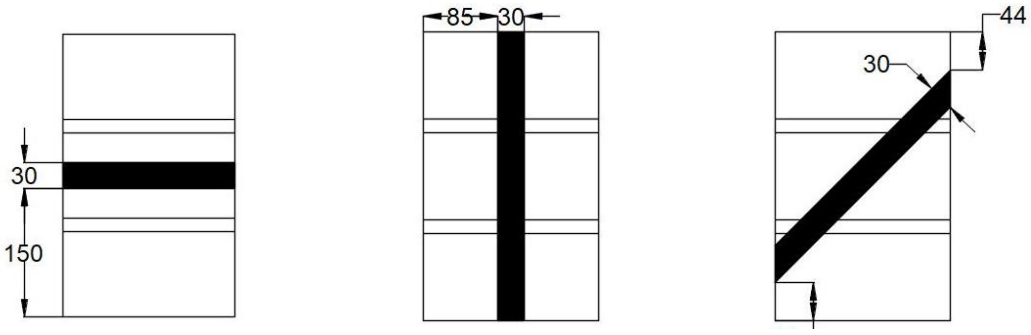

(a) (b) (c)

Fig. 4 Chase arrangement in prisms (a) Horizontal chase, (b) Vertical chase and (c) Inclined chase (Note: All dimensions are in mm.)

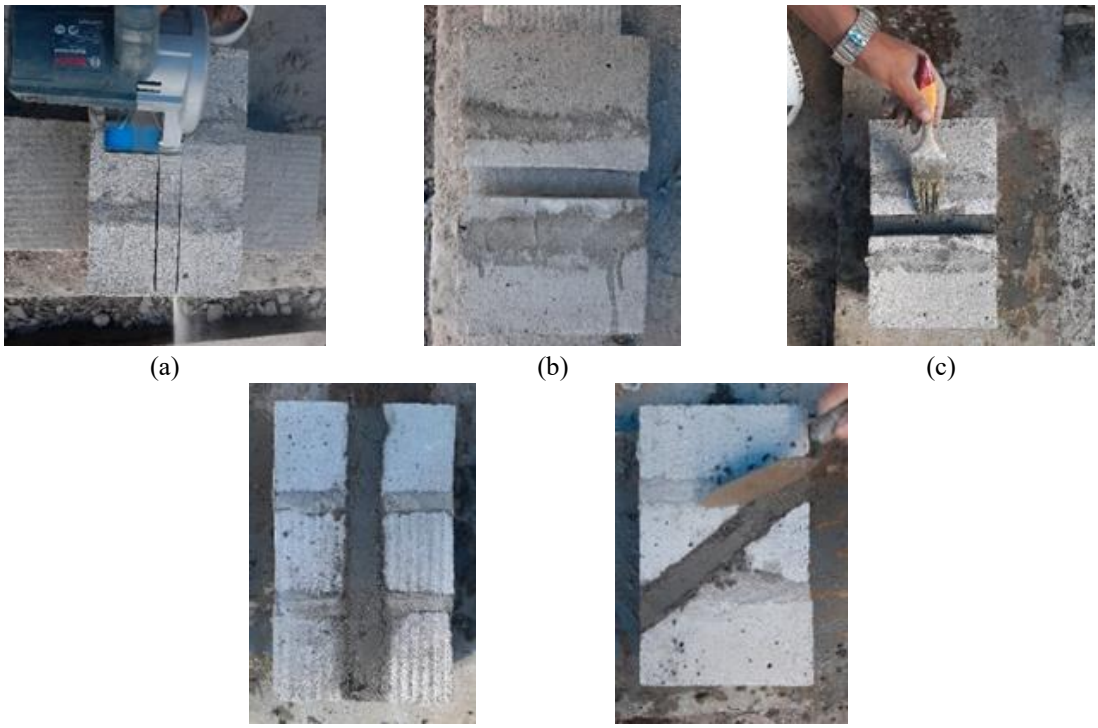

(a) (b) (c)

(d) (e)

Fig. 5 Cutting and filling of chases in prisms (a) Cutting chase using tile cutter, (b) Prism with horizontal chase, (c) Applying cement slurry in chase, (d) Mortar fill in vertical chase and (e) Mortar fill in inclined chase

After the chase cutting phase Fig. 5(a), these grooves were filled with mortars Figs. 5(d) and (e) denoted as S (strong), M (moderate), and W (weak), and the prisms were left to undergo an additional 28 days of curing before progressing to the testing phase. The total number of cast prisms amounted to 37, comprising one control specimen without a chase and 12 specimens each for horizontal, vertical, and inclined chases. Among the 12 specimens for each configuration and depth size, only 9 were filled with mortar. Refer to Table 2 for a detailed description of the masonry prisms.

Table 2 Details of specimens

Specimen Notation	Chase Configuration	Chase Depth	Mortar Mix
C (Control)	-	-	-
H10	Horizontal	10	-
HW10			Weak
HM10			Moderate
HS10			Strong
H20		20	-
HW20			Weak
HM20			Moderate
HS20			Strong
H30		30	-
HW30			Weak
HM30			Moderate
HS30			Strong
V10	Vertical	10	-
VW10			Weak
VM10			Moderate
VS10			Strong
V20		20	-
VW20			Weak
VM20			Moderate
VS20			Strong
V30		30	-
VW30			Weak
VM30			Moderate
VS30			Strong
I10	Inclined	10	-
IW10			Weak
IM10			Moderate
IS10			Strong
I20		20	-
IW20			Weak
IM20			Moderate
IS20			Strong
I30		30	-
IW30			Weak
IM30			Moderate
IS30			Strong

Fig. 6 Test set-up for compression of specimens

(a) (b) (c)

Fig. 7 Failure pattern of control specimen (a) Diagonal crack at face of specimen, (b) Vertical cracks along width of specimen and (c) Vertical cracks along with cracks along bed joint

2.3 Test set up

Following the curing process, the masonry prisms underwent compression testing, adhering to the specifications outlined in ASTM C1314 - 09 (2015). The compression tests were conducted using a Compression Testing Machine (CTM) that complies with IS 14858 2000, calibrated with an accuracy of ± 1%, and possessing a capacity of 3000 kN. The test set-up for compression is shown in Fig. 6.

3. Results and discussions

3.1 Failure mode

The observed failure pattern for the control specimen manifested at the prism's face, characterized by a diagonal crack emanating from the interface between the mortar and block. Simultaneously, on the prism's side, the formation of vertical cracks was observed, as illustrated in the accompanying Fig. 7. This failure mode is indicative of a structural response wherein stress concentration at the mortar-block interface initiates diagonal cracking.

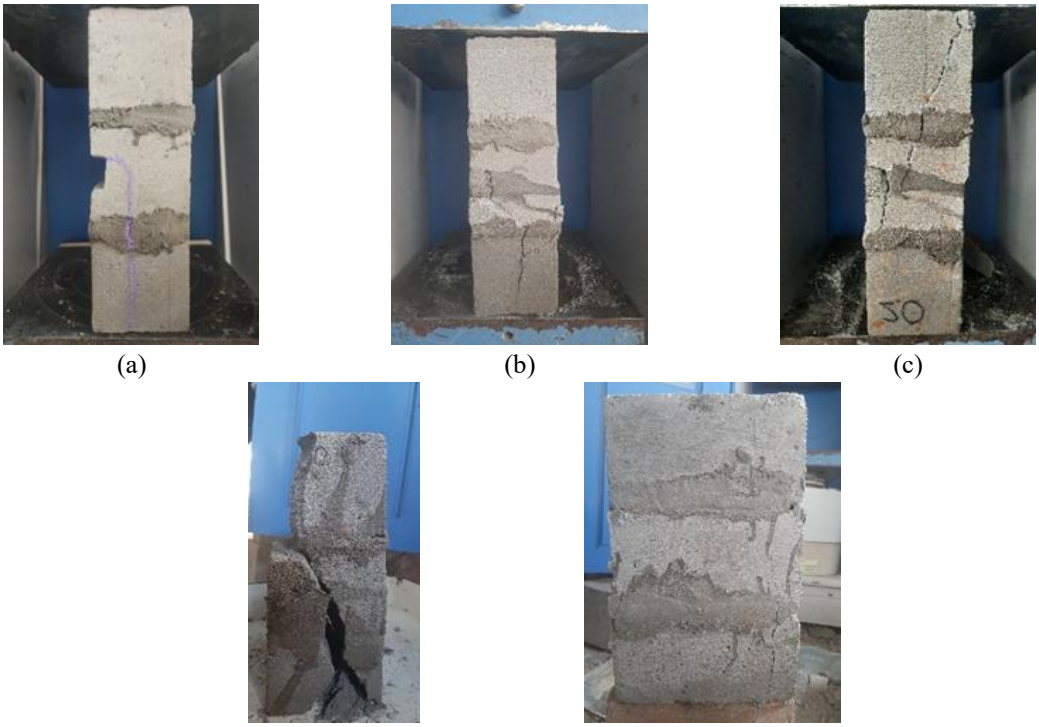

(a) (b) (c)

(d) (e)

Fig. 8 Failure pattern of specimens with horizontal chases (a) Vertical crack propagating from chase in H10, (b) Cracks propagating from chase towards the width of specimen HM10, (c) Diagonal crack propagating from chase HM20, (d) Splitting of prism HS20 and (e) Verticals cracks at bottom of specimen HW30

In prisms featuring horizontal chases, vertical cracks are evident both at the base and the top of the specimens without infill, aligned with the direction of the applied load, Fig. 8(a) shows the crack pattern of specimen H10, a distinct horizontal crack is observed along the chase, propagating to the width of the specimen vertically. In some instances, cracks extend diagonally from the filling mortar in the chase to the base as seen in Fig. 8(b) for specimen HM10, which may result in prism splitting in some specimens like HS20, as illustrated in Fig. 8(d). Other specimens like Fig. 8(c) (specimen HM20), exhibit cracks propagating diagonally upwards from the chase. Specimen HW30 as shown in Fig. 8(e), exhibits vertical cracks at the bottom of the specimen. The most common failure mode for prisms with horizontal chase were vertical cracks at width of the prism propagating from the chase as indicated in Table 3 which aligns with the findings of other researchers such as Mojsilović (2011) and Fleith de Medeiros *et al.* (2022b). They also identified vertical cracks as the predominant failure patterns in their specimens.

In prisms featuring inclined chases, the majority of specimens exhibited face shell separation, as depicted in Figs. 9(b) and (d) showcasing specimen IS30 and IS20 undergoing this separation. Diagonal cracks frequently appeared on the face opposite to the chases and along the chase itself, with these cracks extending to the sides of the prism, resulting in specimen splitting. Vertical cracks and toe crushing, shown in Fig. 9(e) for the specimen IM20 was a common observation. In instances where the chases were filled with a 1:2 mortar mix, complete separation of the mortar from the prism occurred at the ultimate load. Cracks in the mortar of chases are evident in most cases like Fig. 9(c)

Table 3 Failure mode of specimens

Specimen Name	Ultimate Load Capacity (kN)	Failure Mode
C	84.2	Diagonal and vertical cracks, crack at mortar-block interface
H10	57.9	Vertical cracks at width of prism propagating from chase
HW10	59.0	Vertical cracks at width of prism propagating from chase
HM10	62.8	Vertical cracks at width of prism propagating from chase
HS10	69.6	Cracks at mortar-block interface
H20	46.0	Vertical cracks at width of prism propagating from chase
HW20	47.2	Vertical cracks at width of prism propagating from chase
HM20	52.7	Diagonal cracks at width of prism propagating from chase
HS20	55.1	Splitting of prism
H30	43.9	Vertical cracks at width of prism propagating from chase
HW30	45.3	Vertical cracks, splitting of prism
HM30	47.8	Vertical cracks at face of prism
HS30	53.1	Vertical cracks at width of prism propagating from chase
V10	61.2	Diagonal crack at back of prism
VW10	63.6	Diagonal crack at back of prism
VM10	66.7	Cracks along chase and along binding mortar
VS10	70.4	Cracks along chase, block crushing at bottom of prism
V20	49.7	Cracks along chase
VW20	51.5	Cracks along chase and block crushing at top of prism
VM20	52.4	Cracks along chase
VS20	54.0	Block crushing
V30	35.4	Cracks along chase
VW30	38.1	Cracks along chase and block crushing at top of prism
VM30	40.6	Splitting of prism along chase
VS30	43.8	Debonding of mortar from chase, diagonal crack along width
I10	51.6	Cracks along chase
IW10	54.2	Diagonal cracks along width
IM10	59.8	Crack along block-mortar interface, block crushing
IS10	72.7	Face-shell separation, crack along infill mortar
I20	41.6	Cracks along chase
IW20	41.9	Cracks along chase
IM20	45.0	Vertical crack along width of prism, toe crushing
IS20	47.7	Face-shell separation
I30	30.8	Cracks along chase
IW30	35.0	Vertical cracks at front face, diagonal cracks at back
IM30	38.7	Crack at infill mortar, cone and split failure
IS30	44.6	Face-shell separation, crack along infill mortar

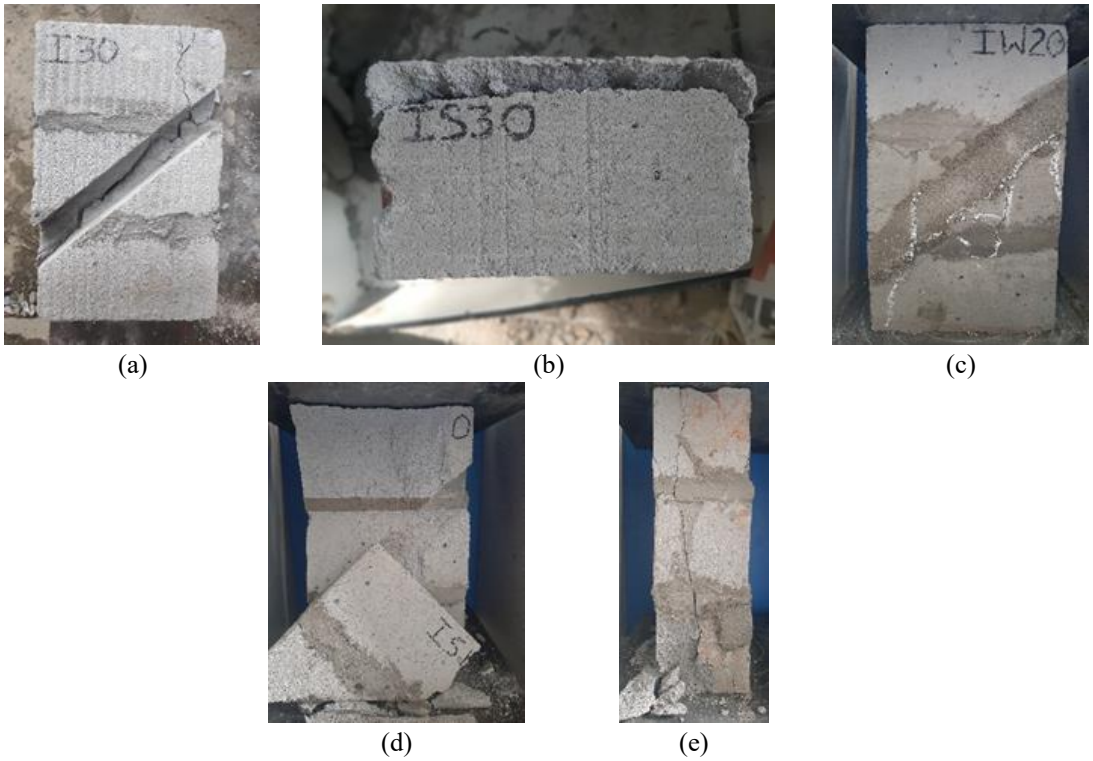

Fig. 9 Failure pattern of specimens with inclined chases (a) Crack along chase I30, (b) Face shell separation IS30, (c) Cracks along the chase IW20, (d) Face shell separation IS20 and (e) Vertical crack and toe crushing IM20

showing specimen IW20 where these cracks propagate to the bricks along the chase configuration. In specimens without chase fill like Fig. 9(a) showing specimen I30, the cracks are distinctly visible along the chase.

In prisms with vertical chases, vertical cracks form along the chase as shown in Fig. 10(a) (VS10) and propagating diagonally on the face of the prism. Block crushing is a common outcome, as depicted in the Figs. 10(c) and (d) (VS20 and VW30). Specimen VM30, Fig. 10(b), undergoes complete splitting along the chase at the ultimate load, reflecting the findings of Mojsilović (2011) for specimens with vertical chases. Similar to inclined chases with strong mortar, prisms with strong mortar entirely debond from the prism and undergo tensile splitting, as depicted in Fig. 10(f), showing specimen VS30 with the filling mortar debonding and splitting in the middle. Vertical cracks formed at the top of the specimen that propagates to the bonding mortar as well as vertically down, depicted in Fig. 10(e) (VM10) is also a common pattern. For prisms with no fill in chases, vertical cracks were observed to have formed along the chase.

The failure mode observed in this study, especially for specimens with horizontal chases aligns with findings from other authors such as Fleith de Medeiros *et al.* (2022b) and Mojsilović (2011), who noted vertical cracks and specimen splitting as predominant failure patterns. Similarly, Al-Sibahy and Edwards (2021) also observed crack formations along chases in their study. Furthermore, the failure modes align with Milani *et al.* (2021) on small-scale clay block masonry walls with chases under compression where chase cuts cause cracks that split the block surface and extend vertically

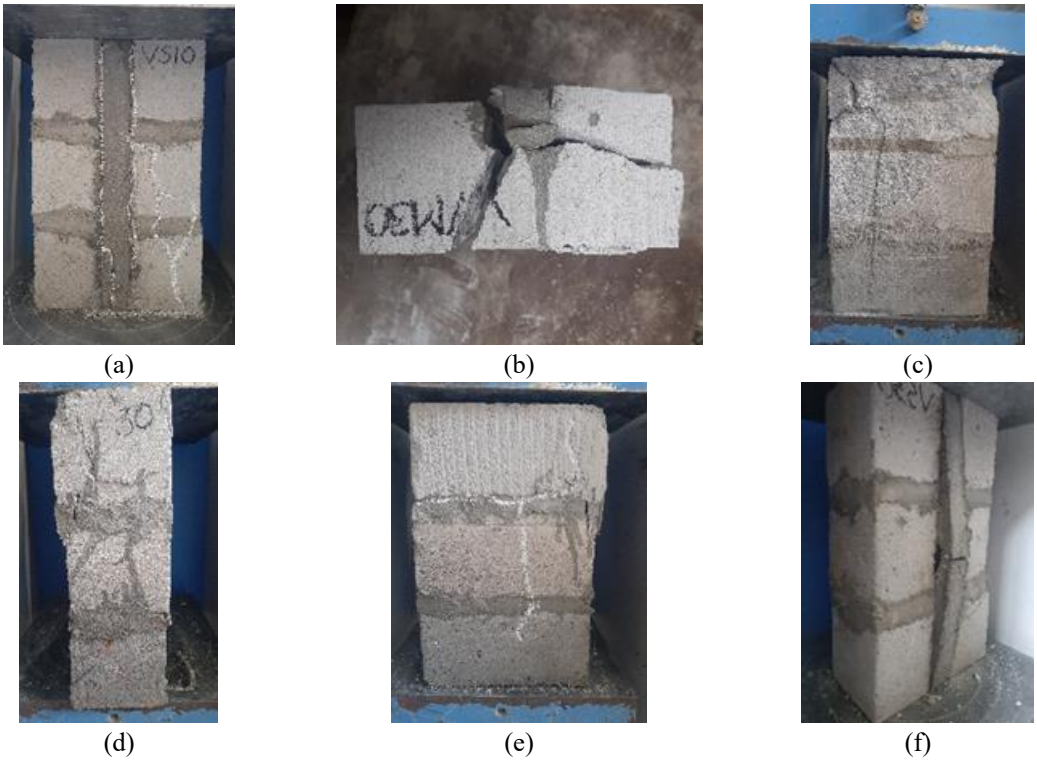

Fig. 10 Failure pattern of specimens with vertical chases (a) Vertical cracks along chase propagating diagonally at face VS10, (b) Splitting of prism along chase VM30, (c) Block crushing VS20, (d) Block crushing at top along width VW30, (e) Vertical crack and crack along binding mortar VM10 and (f) Debonding of mortar from chase VS30

to the block-mortar interface leading to tensile stress loss of adhesion and masonry failure.

3.2 Ultimate load capacity (P_{max})

This section discusses the ultimate load capacities of prisms based on their configuration, chase depth, and fill type. The control specimen exhibited a peak load of 84.2 kN. Results from the Compression Testing Machine reveal that the prisms with chases generally have a lower load-carrying capacity compared to the control specimen.

For prisms with horizontal chases, the maximum load (P_{max}) varied between 43 kN and 58 kN, depending on both the depth of the chase and the type of mortar used for filling. Prisms with larger chase depths exhibited lower load capacities, and those filled with stronger mortar demonstrated higher load capacities than those with moderate or weak mortar. For instance, HW20 and HW30 (H-Horizontal, W-Weak) had P_{max} values of 52.4 kN and 45.2 kN, respectively. This indicates that the prism with a 30 mm chase depth had a lower load capacity than the one with a 20 mm chase depth. In another comparison, between HW30 and HS30, P_{max} values were 45.2 kN and 53.1 kN, respectively, highlighting that the prism filled with strong mortar had a higher load capacity than the one filled with weak mortar.

Regarding vertical chases, P_{max} ranged from 35 kN to 70 kN. The VS10 specimens recorded the

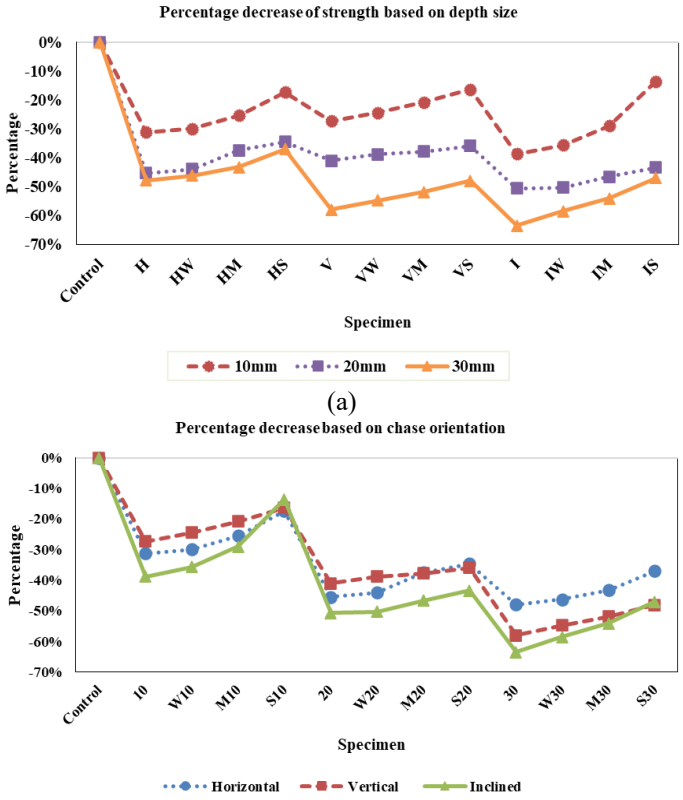

Fig. 11 Percentage decrease in compressive strength based on (a) Size of chase depth and (b) Orientation of chase

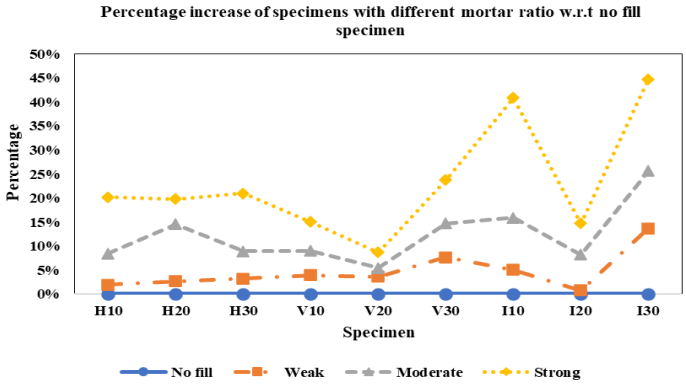

Fig. 12 Percentage increase in compressive strength of specimens with infill material w.r.t no fill specimens

highest load capacity at 70.4 kN, while the V30 specimen recorded the lowest load capacity, supporting the theory that chases with greater depth results in lower compressive strength. The percentage increase in compressive strength for prisms with infill material in the chase compared to those with only a chase and no filling material ranged from 3% to 24%. Notable, VS30 exhibited

the highest increase in compressive strength at 23.73%. Overall, the compressive strength of vertical chases was comparatively higher than that of horizontal chases.

For prisms with inclined chases, P_{max} ranged from 30 kN to 73 kN. These prisms showed a wider range of strength between specimens compared to vertical and horizontal chases. The compressive strength of inclined chases with no fill, weak mortar, and moderate-strength mortar was lower than that of both vertical and horizontal chases. However, when the chase had strong mortar embedded, the inclined chase demonstrated a higher compressive strength than both horizontal and vertical chases. It can also be observed that there was no proportional increase in resistance for prism with vertical and incline chase. This lack of proportion can be attributed to the stress concentration at the block-mortar interface, which creates discontinuity, even when filled with mortar, preventing uniform load distribution as in a solid prism. Additionally, the observed variation may be due to the low number of samples used in the study, with only one specimen for each evaluated group. Similar to horizontal and vertical chases, the compressive strength of specimens increased with strong mortar and decreased with the chase depth size. The increase in strength compared to the chase with no fill ranged from 0.7% to 45%.

Figs. 11(a) and (b) presents the graphical representation of the percentage decrease in compressive strength of the specimens based on chase depth size and chase orientation respectively and Fig. 12. presents the graphical representation of the percentage increase in compressive strength of specimens with infill material w.r.t no fill specimens.

4. Conclusions

The investigation into the compressive behavior of masonry prisms featuring chases has been carried out with the goal of comprehending how these structural elements impact overall masonry performance. In this current study, the objective was to explore the influence of various chase configurations, chase depths, and infill mortar on the compressive strength of AAC masonry prisms. To achieve this, 37 specimens were prepared, with one serving as a control, while the others featured three distinct configurations (horizontal, vertical, and inclined), varied depth sizes (10mm, 20mm, and 30mm), and different infill mortar types; some specimens were left unfilled. All specimens underwent testing using a Compression Testing Machine (CTM).

The following conclusions are drawn from the conducted experiment:

i. Findings from various studies (Fleith de Medeiros *et al.* 2022a, Mojsilović 2011) align with the noticeable decrease in the compressive strength of masonry due to the introduction of chases.

ii. The overall reduction in compressive strength ranges from 13% to 63%, signifying a substantial impact.

iii. Depth impact

• The depth of the chase plays a pivotal role, with a 10 mm depth chase exhibiting a lesser reduction in strength compared to 20 mm and 30 mm depths.

• Specifically, the strength reduction in 20 mm and 30 mm depth chases falls within comparable ranges, ranging from 34% to 51% for 20 mm depth and 35% to 58% for 30 mm depth.

iv. Configuration Impact:

• Disparity in strength reduction is less apparent based on configuration.

• Prisms with horizontal, vertical, and inclined chases exhibit compressive strength reductions between 17% and 48%, 22% and 58%, and 13% and 64%, respectively, compared to the control specimen.

v. Influence of Mortar Mix:
• Unlike Mojsilović (2011), the choice of mortar mix for filling the chase has a discernible impact on strength reduction.
• Prisms filled with higher-strength mortar show less reduction in overall specimen strength.
• Prisms with a 1:2 mix mortar display significantly higher compressive strength than specimens without chase fill, highlighting the crucial role of mortar composition in determining masonry strength. This contrasts with Vicente *et al.* (2014), where specimens with inclined chases did not experience a strength increase even after filling the chase with mortar, while horizontal and vertical chase specimens did show an increase in strength compared to those without chase infill.
• Overall, it is evident that to prevent a significant loss of strength in elements with chases, the infill should be at least as strong and stiff as the masonry unit (Mojsilović 2011).

Future scope

In this study, the chases were filled with mortar to focus on the effect of the grooves on structural stability. However, this approach is not entirely practical, as real-world scenarios typically involve installing pipes for wiring or plumbing. Future research could extend the study by including the installation of pipes in the chases and sealing them before testing, offering a more practical and accurate assessment. Additionally, it is important to note that the observed values refer to the analysis of the prisms. However, on a full wall, the results would likely vary in numerical terms, though the observed trends would remain consistent. Therefore, it is recommended to expand this study to full-scale masonry wallets to further analyze the effect of grooves on structural stability.

References

Al-Sibahy, A. and Edwards, R. (2021), "Effect of chases with renovation techniques on the load carrying capacity of masonry walls", *Infrastr.*, **6**, 160. https:// doi.org/10.3390/infrastructures6110160.

ASTM C1314-09 (2015), Standard Test Method for Compressive Strength of Masonry Prisms, ASTM International, West Conshohocken, PA, USA.

British Standard EN 1996-1-1 (2005), Eurocode 6: Design of Masonry Structures - Part 1-1: General Rules for Reinforced and Unreinforced Masonry Structures, The British Standards Institution, London, UK.

Banerjee, S., Nayak, S. and Das, S. (2019), "Enhancing the flexural behaviour of masonry wallet using PP band and steel wire mesh", *Constr. Build. Mater.*, **194**, 179-191. https://doi.org/10.1016/j.conbuildmat.2018.11.001.

Bhosale, A., Zade, N.P., Davis, R. and Sarkar, P. (2019), "Experimental investigation of autoclaved aerated concrete masonry", *J. Mater. Civil Eng.*, **31**(7), 04019109. https://doi.org/10.1061/(asce)mt.1943-5533.0002762.

Costigan, A. and Pavía, S. (2009), "Compressive, flexural and bond strength of brick/lime mortar masonry", *Proceedings of PROHITEC 09*, Rome, Italy, June.

de Medeiros, G.F., Mohamad, G., Kosteski, L.E., Rodriguez, R.Q. and Milani, A.S. (2022a), "Strength capacity of hollow clay blocks structural masonry - Flange, Chases, and slenderness effects", *Eng. Struct.*, **272,** 114943. https://doi.org/10.1016/j.engstruct.2022.114943.

de Medeiros, G.F., Milani, A.S., Lubeck, A., Mohamad, G., Rodriguez, R.Q. and Kosteski, L.E. (2022b), "Numerical analysis of masonry walls with horizontal chases using the Lattice Discrete element method (LDEM)", *Eng. Struct.*, **253**, 113647. https://doi.org/10.1016/j.engstruct.2021.113647.

Eurocode 6. EN 1996-1-1 (2005), Design of Masonry Structures - Part 1-1: Common Rules for Reinforced

and Unreinforced Masonry Structures, Brussels, Belgium.
Ferretti, D. and Michelini, E. (2021), "The effect of density on the delicate balance between structural requirements and environmental issues for AAC blocks: An experimental investigation", *Sustain.*, **13**(13186), 1-21. https://doi.org/10.3390/su132313186.
Ferretti, D., Michelini, E. and Rosati, G. (2015), "Mechanical characterization of autoclaved aerated concrete masonry subjected to in-plane loading: Experimental investigation and FE modeling", *Constr. Build. Mater.*, **98**, 353-365. https://doi.org/10.1016/j.conbuildmat.2015.08.121.
Gumaste, K.S., Nanjunda Rao, K.S., Venkatarama Reddy, B.V. and Jagadish, K.S. (2007), "Strength and elasticity of brick masonry prisms and wallettes under compression", *Mater. Struct.*, **40**, 241-253. https://doi.org/10.1617/s11527-006-9141-9.
Hendry, E.A.W. (2001), "Masonry walls: Materials and construction", *Constr. Build. Mater.*, **15**, 323-330. https://doi.org/10.1016/S0950-0618(01)00019-8.
IS 14858 (2000), Requirements for Compression Testing Machine Used for Testing of Concrete and Mortar, Bureau of Indian Standards (BIS), New Delhi, India.
IS 1905 (1987), Code of Practice for Structural Use of Unreinforced Masonry, Bureau of Indian Standards (BIS), New Delhi, India.
IS 383 (1970), Specification for Coarse and Fine Aggregates From Natural Sources for Concrete, Bureau of Indian Standards (BIS), New Delhi, India.
IS 4031 (Part 6) (1988), Determination of Compressive Strength of Hydraulic Cement Other than Masonary Cement, Bureau of Indian Standards (BIS), New Delhi, India.
Kałuza, M. (2017), "Analysis of in-plane deformation of walls made using AAC blocks strengthened by GFRP mesh", *Procedia Eng.*, **193**, 393-400. https://doi.org/10.1016/j.proeng.2017.06.229.
Lyngkhoi, R.B., Warjri, T. and Marthong, C. (2023), "Shear performance of AAC masonry triplets strengthened by reinforcing steel wire mesh in the bed and bed - head joint", *Earthq. Struct.*, **25**(3)**,** 149-160. https://doi.org/10.12989/eas.2023.25.3.149.
Michelini, E., Ferretti, D., Miccoli, L. and Parisi, F. (2023), "Autoclaved aerated concrete masonry for energy efficient buildings: State of the art and future developments", *Constr. Build. Mater.*, **402**, 132996. https://doi.org/10.1016/j.conbuildmat.2023.132996.
Milani, A.S., Lübeck, A., Mohamad, G., Neto, A.B.D.S.S. and Budny, J. (2021), "Experimental investigation of small-scale clay blocks masonry walls with chases under compression", *Constr. Build. Mater.*, **273**, 121539. https://doi.org/10.1016/j.conbuildmat.2020.121539.
Mojsilović, N. (2011), "Masonry elements with chases: Behaviour under compression", *Constr. Build. Mater.*, **25**, 4415-4425. https://doi.org/10.1016/j.conbuildmat.2010.12.027.
Narayanan, N. and Ramamurthy, K. (2000), "Structure and properties of aerated concrete: A review", *Cement Concrete Compos.*, **22**, 321-329. https://doi.org/10.1016/S0958-9465(00)00016-0.
Raj, A., Borsaikia, A.C. and Dixit, U.S. (2020a), "Bond strength of Autoclaved Aerated Concrete (AAC) masonry using various joint materials", *J. Build. Eng.*, **28**, 101039. https://doi.org/10.1016/j.jobe.2019.101039.
Raj, A., Borsaikia, A.C. and Dixit, U.S. (2020b), "Evaluation of mechanical properties of autoclaved aerated concrete (AAC) block and its masonry", *J. Inst. Eng. Ser. A*, **101**(2), 315-325. https://doi.org/10.1007/s40030-020-00437-5.
Sathiparan, N. and Rumeshkumar, U. (2018), "Effect of moisture condition on mechanical behavior of low strength brick masonry", *J. Build. Eng.*, **17**, 23-31. https://doi.org/10.1016/j.jobe.2018.01.015.
Singh, S.B. and Munjal, P. (2017), "Bond strength and compressive stress-strain characteristics of brick masonry", *J. Build. Eng.*, **9**, 10-16. https://doi.org/10.1016/j.jobe.2016.11.006.
Vicente, R., Varum, H., Figueiredo, A., Ferreira, T.M. and Mendes da Silva, J.A.R. (2014), "Hollowed clay brick masonry elements with chases: Behaviour under compression", *9th International Masonry Conference*, Guimaraes, Portugal, July.